Journal of Photochemistry & Photobiology A: Chemistry 382 (2019) 111878

Contents lists available at ScienceDirect

Journal of Photochemistry & Photobiology A: Chemistry

journal homepage: www.elsevier.com/locate/jphotochem

Synthesis of carbon nanohoops containing thermally stable cis azobenzene

Paul J. Evans[a], Lev N. Zakharov[b], Ramesh Jasti[a,*]

[a] Department of Chemistry and Biochemistry, University of Oregon, Eugene, OR 97403, United States
[b] CAMCOR, University of Oregon, Eugene, OR 97403, United States

ARTICLE INFO

Dedicated to Rajendra Rathore.

Keywords:
Cycloparaphenylene
Macrocycles
Azobenzene
Supramolecular chemistry
Host-guest chemistry
Synthesis

ABSTRACT

Cycloparaphenylenes (CPPs) have been praised for their size-tunable HOMO/LUMO gap and associated electronic and optical properties, and have generated significant interest for small-molecule electronics. Another fascinating but less-explored prospect for CPPs involves exploiting their hollow geometry. With a rigid pore of tunable size and high electron density arising from the inward facing π-orbitals, CPPs are ideal for electron-poor guests. [10]CPP in particular has shown very high binding affinity for fullerene C60. The ability to reverse this encapsulation by external stimuli is an important next step. Herein we report the design and synthesis of two CPPs containing thermally stable *cis* azobenzene moieties in the conjugated framework, their behavior upon irradiation, and computational results evaluating their potential as photoswitchable fullerene hosts.

1. Background and synthetic design

Hydrocarbon macrocycles with inward facing π-orbitals have established utility as molecular containers. The rigid, circular, electron-rich pores in cycloparaphenylacetylenes (CPPAs) and cycloparaphenylenes perfectly complement the convex electron-poor exterior of fullerenes [[1]]. [6]CPPA and [10]CPP in particular form strong host-guest complexes with buckminsterfullerene C_{60} [1a,2]. CPPs and related carbon nanohoops can also encapsulate C_{70} and metallofullerenes like Gd@C_{82} and Li@C_{60} [3]. Indeed, these π-π interactions can be quite strong. One of the strongest fullerene hosts, with a remarkable log K_a of 9.7 in dichloromethane, is a benzannulated carbon nanohoop synthesized by Isobe and coworkers [4].

High binding affinity is only one of a set of desirable features in a molecular container. The ability to capture and release a guest has obvious usefulness for the reversible encapsulation and separation of molecules via supramolecular interactions. One approach that has been widely applied is the incorporation of a photoswitchable moiety into the framework of the container [5]. Taking advantage of the *cis-trans* photoisomerization of azobenzene has proved to be one of the simplest and most effective ways to open and close molecular containers such as cyclodextrins [6], crown ethers [7], dendrimers [8], cavitands [9], cryptands [5], and calixarenes [10]. Thus, we took interest in the incorporation of azobenzene into the CPP scaffold and herein report the synthesis of two sizes of bent phenylene nanohoops with an azo moiety (azo[n]CPPs), their structure and irradiation studies.

2. Structural analysis by density functional theory (DFT)

To assess the feasibility of this system we first investigated potential targets by DFT. Adopting a teardrop geometry, *cis*-azo[11]CPP (Fig. 1) has a narrower cavity than circular *trans* conformation (13.0 Å at its narrowest diameter versus 15.7 Å in *trans*-azo[11]CPP based on B3LYP/6-31G* calculations [11]). Irradiation, in principle, would allow for the control of the ratio of these “closed” and “open” hoops and therefore the capture and release of suitably-sized guests. Calculations predict a small 0.4 kcal/mol ground state energy difference favoring the *cis* form. Electronically, owing to a stabilized LUMO, which resides on the azo moiety (supporting information, Figs. S11, S12, S15 and S16 and accompanying details) the azo[*n*]CPP isomers have slightly smaller HOMO-LUMO gaps than a CPP of corresponding size, for example: 3.01 eV and 2.88 eV respectively for *cis*- and *trans*-azo[11]CPP and 3.61 eV for [12]CPP and 3.06 eV and 2.89 eV for *cis*- and *trans*-azo [9]CPP while [10]CPP has a HOMO-LUMO gap of 3.53 eV [12]. Thus, it seems that the strain from deforming the oligophenylene does not threaten significantly the stability of either isomer and the inclusion of the azo moiety will not disrupt the electronics to instability, making the azo[*n*]CPPs fascinating and obtainable synthetic targets.

3. Synthesis of azo[11]CPP

The synthesis of a nine-ring diboronate **1** was accomplished in five steps from commercially available material (details in supporting information Scheme S2). The desired macrocycle **3** was formed in 13%

* Corresponding author.
E-mail address: rjasti@uoregon.edu (R. Jasti).

https://doi.org/10.1016/j.jphotochem.2019.111878
Received 13 November 2018; Received in revised form 6 April 2019; Accepted 28 May 2019
Available online 31 May 2019
1010-6030/

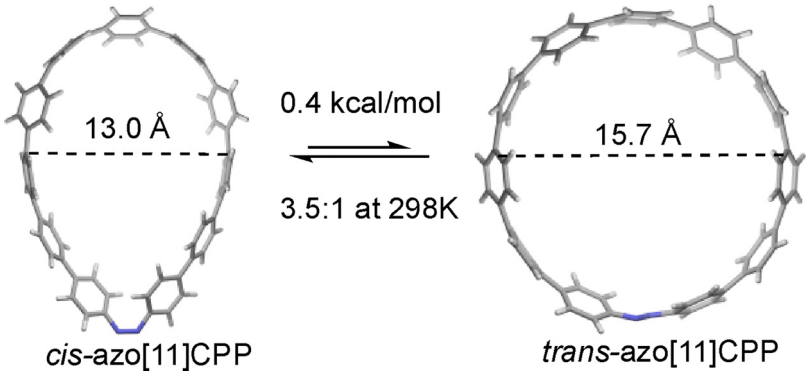

Fig. 1. DFT structures of *cis*- and *trans*-azo[11]CPP.

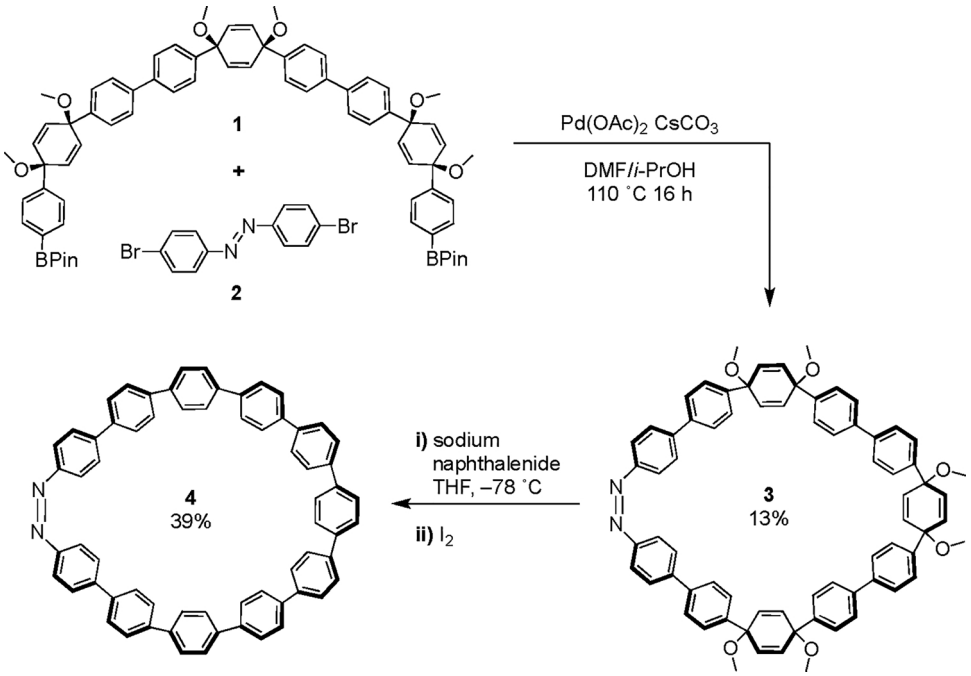

Fig. 2. Synthesis of azo[11]CPP.

yield from **1** and 4,4′-dibromoazobenzene, **2**. Sodium naphthalenide mediated reductive aromatization proceeded cleanly to give the desired nanohoop, azo[11]CPP, **4**, as a bright orange solid (Fig. 2). An upfield doublet in the ^{1}H NMR spectrum (δ = 6.90 ppm) corresponds to the four protons closest to the nitrogen atoms in a *cis*-azobenzene moiety that lie in the shielding cone of the opposite azobenzene aryl ring and indicates that the *cis* orientation dominates in solution (δ = 6.82 ppm for a *cis* compound in Ref. 13). No NMR evidence of a *trans* isomer was apparent. Since the DFT modelization only predicted a small difference in energy between the isomers, it seems likely that solvent reorganization may contribute to the stability of the *cis* isomer. Thermally stable *cis* azobenzenes of this type are rare, but not unknown [13,14]. Attempts were also made to use oxidative azobenzene formation as an intramolecular macrocyclization from a corresponding curved dianiline analog of **1**. However, this electron-rich precursor proved to be unstable in solution and this approach was abandoned.

4. Design of smaller azoCPPs

To provide a meaningful geometric comparison to azo[11]CPP, we targeted the much smaller and therefore more strained azo[7]CPP. Intermolecular macrocyclization was attempted with dibromoazobenzene **2** and the same five-ring diboronate **5** that furnished [5]CPP [15]. However, it was determined that the major cyclic product of this reaction was the hourglass-shaped all-*trans* diazobenzene macrocycle **6** arising from the coupling of two equivalents of **5** with two equivalents of **2**. X-ray Diffraction Crystallography (XRD) confirmed this structure and showed that the azobenzene nitrogen-nitrogen double bonds are in close contact (3.2 Å) in the solid state (Fig. 3). Additionally, these inherently chiral molecules pack tightly into a solvent-free lattice as a racemic mixture.

When a solution of **6** is irradiated with 360 nm LED light (360 nm, 800 mW), the three-state switching between *trans-trans*, *cis-trans*, and *cis-cis* macrocycles is observed by ^{1}H NMR (supporting information Fig. S1). Owing to the high molecular weight and calculated flattened all-*cis* structure of the expected oligophenylene product (supporting information Fig. S14), the treatment of **6** with sodium naphthalenide returned a fluorescent yellow-orange solid that was extremely insoluble and amorphous, thus uncharacterizable by NMR or XRD.

We reasoned, having seen the success of the azo[11]CPP synthesis and the dimerization of the macrocyclization en route to azo[7]CPP, that more curvature in the diboronate would encourage bimolecular macrocyclization and discourage higher-order cyclic oligomers. In computational investigations of unknown azo[*n*]CPPs, it came to light that one size in particular, azo[9]CPP may have an affinity for C_{60} due to its similar diameter to [10]CPP. When measured centroid-to-centroid

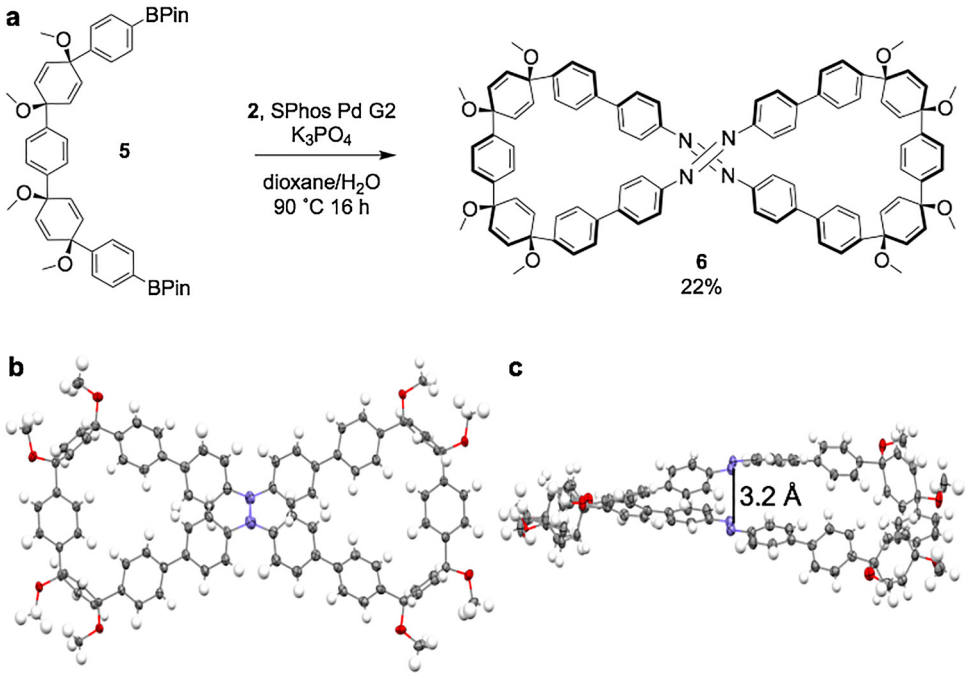

Fig. 3. Synthesis (a) and crystal structure top (b) and side view (c) of dimeric macrocycle **6**.

[10]CPP has a diameter of 13.5 Å in the solid state and binds C_{60} with a log K_a of 6.4 [2a]. The minimized geometry of *trans*-azo[9]CPP, meanwhile is just slightly smaller, with an average diameter of 13.2 Å (supporting information, Fig. S2). This is the same as Kawase's [6]CPPA that binds C_{60} with a log K_a of 4.2 [16]. Given the enhanced π-density in the cycloparaphenylene, the binding of *trans*-azo[9]CPP is expected to be intermediate between these two nanohoops.

To validate the feasibility of this nanohoop as a molecular container for C_{60}, *ab initio* calculations at the M062X/6-31G* level were conducted [11]. The ground state energy climb from *cis* to *trans* using this basis set was calculated to be 1.27 kcal/mol, slightly less than the 2.12 kcal/mol difference as calculated using B3LYP/6-31G*. However both of these energies are small compared to the 34.32 kcal/mol heat of formation of the ball-in-bowl complex of C_{60} with *trans*-azo[9]CPP (Fig. 4). The isomerization of azobenzene is known for overcoming significant strain [13] including isomerization barriers of 34 kcal/mol [17]. Therefore, assuming that these states are in equilibrium and the barriers between them are accessible under experimental conditions *trans*-azo[9]CPP should form a strong association with C_{60}, and the complex will be the major thermodynamic product. It should be noted that M062X/6-31G* is known to overestimate the energy gained in such complexations but serves to make comparisons between systems [2a].

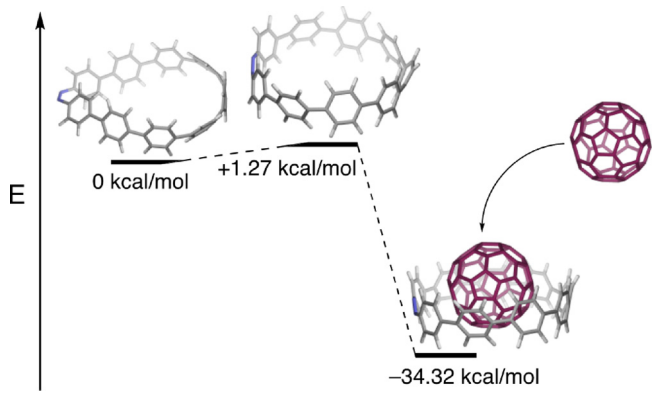

Fig. 4. M062X/6-31G* energies for azo[9]CPP and *trans*-azo[9]CPP@C_{60}.

For example, with the same basis set the heats of formation of C_{60} complexes with [10]CPP and [6]CPPA were calculated to be 41.35 kcal/mol and 28.0 kcal/mol respectively [2a,18]. Solvent was excluded in calculations here and those known in the literature, though it no doubt has a role, this keeps comparisons of data relevant. With a heat of formation lying between those of two known fullerene hosts, these computational data provide a firm theoretical foundation for our choice to synthesize azo[9]CPP.

5. Synthesis of azo[9]CPP

For the synthesis of azo[9]CPP, a new diboronate **7** was synthesized in 22% yield over three steps (details in supporting information Scheme S3). The tight curvature and few degrees of rotational freedom in **7** provide a platform for the synthesis of new CPPs via intermolecular coupling with flat coupling partners. It was discovered that **7** will undergo Suzuki macrocyclization with dibromoazobenzene **2**, which lies preferentially in the linear *trans* conformation in solution (Fig. 5). Purification of the reaction mixture by preparative GPC provided macrocycle **8** in a 22% isolated yield as orange needles. Again we observed only a *cis* isomer in solution (^{1}H NMR doublet, δ = 6.80 ppm).

The identity of the desired macrocycle **8** was further confirmed by XRD (Fig. 6a). In the crystalline state, this molecule has a roughly triangular pore and a steeply-buckled cyclic shape; a curvature which leads to one-dimensional channels of nesting molecules with tetrahydrofuran disordered in the pore (Fig. S10). The benzene rings in the azobenzene moiety are also slightly disordered, adopting a number of conformations. After isolating and confirming the identity of the macrocycle, **8** was subjected to sodium naphthalenide at –78 °C and aromatized to offer azo[9]CPP (**9**, Fig. 5) in 57% yield, with a thermal *cis* conformation confirmed by NMR (doublet, δ = 6.84 ppm) and XRD (Fig. 6b).

6. Photoswitching studies

Having isolated two different sizes of azo[*n*]CPP, we set out to determine the feasibility of switching the pore size of these nanohoops. The UV–vis spectrum of azo[11]CPP (**4**) in CH_2Cl_2 displayed a major absorption at 333 nm and though a minor absorption was apparent

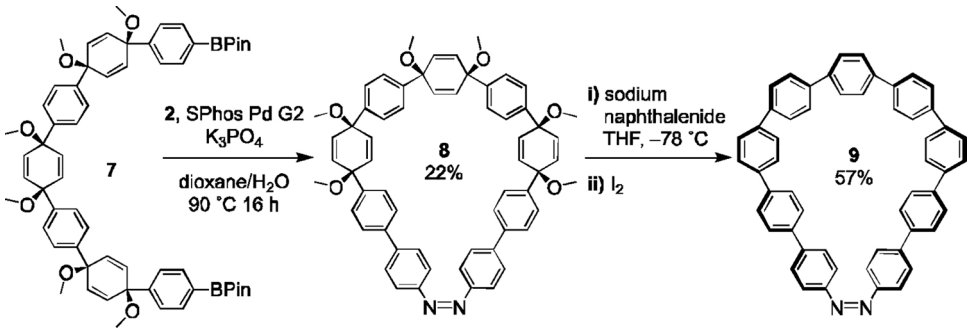

Fig. 5. Synthesis of azo[9]CPP.

further in the red (qualitatively from the orange appearance of the solid and solution and also calculated by TD-DFT [11], Supporting information Fig. S3) increasing the concentration of the sample to observe this peak only resulted in the major absorbance overwhelming the region where a second absorbance was expected. Irradiation of this sample with a 4-watt fluorescent mercury lamp at 365 nm resulted in the depression of the major absorbance and the appearance of a longer wavelength shoulder centered around 370 nm (Fig. 7a). This is likely the major absorption of the *trans* species, which should lie at a longer wavelength than the *cis* as calculated by TD-DFT (supporting information Fig. S3). In fact, the simulation of cyclic azobenzene oligomers shows this absorption behavior upon isomerization from *cis* to *trans* of the azobenzene moieties and even estimates that the inclusion of one *cis* azobenzene in lowers the overall energy of the macrocycle, further supporting the characterization of this as a *cis* to *trans* isomerization [19]. This phenomenon was reversed over fifteen minutes at room temperature under ambient light, with a resulting spectrum identical to the starting material. This switching was repeatable and concentration independent.

When a shorter wavelength was used for irradiation (fluorescent mercury lamp, 4 Ws, 254 nm), the major absorption of the sample was irreversibly blue-shifted and a decrease in total absorbance was observed (Fig. 7b). Additionally, all signals in the ^{1}H NMR spectrum of a sample of **4** disappeared (Fig. S6). After weeks at room temperature and under ambient light or longer wavelength irradiation (365 nm) this sample remained unchanged. In certain cases, thermal azobenzene isomerization can be very slow [10], but the original absorbance of this sample never recovered upon storage in solution.

The irreversible nature of this transformation suggests a photochemical degradation rather than an isomerization. Cyclodehydrogenation of *cis*-azobenzenes to the corresponding benzo[c]cinnolines has been observed under photochemical conditions, though typically these require the addition of a Lewis acid and irradiation of higher power and longer duration than employed here [20]. Nevertheless, the resulting product was soluble and did not exhibit the bright fluorescence of an acyclic oligophenylene, so it is reasonable to assume the degradation was not a ring-opening process. Furthermore, TD-DFT simulation of the benzo[c]cinnoline derivative of *cis*-azo[11]CPP shows a major absorption with a smaller extinction coefficient, as was observed (supporting information Fig. S3). Additionally, the broad longer-wavelength absorption is predicted to disappear, accounting for the pale-yellow color of the photolyzed sample. Of course, other routes of photochemical decomposition cannot be completely ruled out by the available data. The small amount of CPP available from this synthesis precluded further NMR investigation of the photoswitching or photodegradation, and the photodegradation product yielded no clear results in MALDI-TOF mass determination.

The smaller azo[9]CPP (**9**) shows an absorption very similar to azo[11]CPP with a major absorption centered around 330 nm and two absorption shoulders at 390 nm (weak) and a 460 nm (very weak) which are both overwhelmed at high concentrations by the broadened edges of the major absorption (Fig. 8a). This nanohoop, interestingly, does not display the switching behavior seen in the UV–vis of azo[11]CPP. Few azobenzene derivatives have completely frozen isomerization and this usually requires high strain, as from a very small macrocycle [14], or coordination of one or more of the nitrogen atoms [21]. Multiple trials using a fluorescent mercury lamp (4 W) at 365 nm, a high-pressure mercury arc lamp (Oriel, 200 W) and longpass filters with cutoff wavelengths stepping gradually down from 550 nm to 350 nm (Fig. 8a), irradiation with high-intensity LED sources (Engin, 800 mW) at 360, 400, 460, 523, and 660 nm also resulted in spectra identical to the original. When exposed to broadband UV irradiation from a high pressure mercury lamp (IR filter only, Fig. 8b) or 254 nm irradiation from a 4 W florescent source, azo[9]CPP bleached in a manner similar to azo[11]CPP consistent again with the predicted irreversible change in absorption upon benzo[c]cinnoline formation

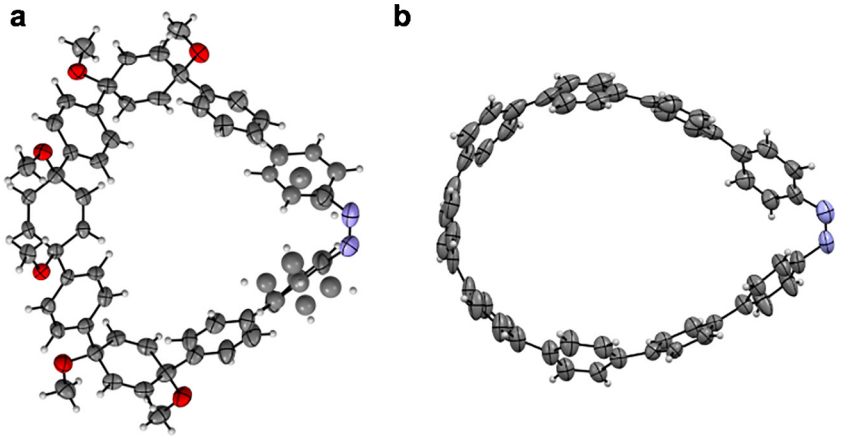

Fig. 6. XRD structures of **8** (a) and **9** (b). Solvent excluded for clarity.

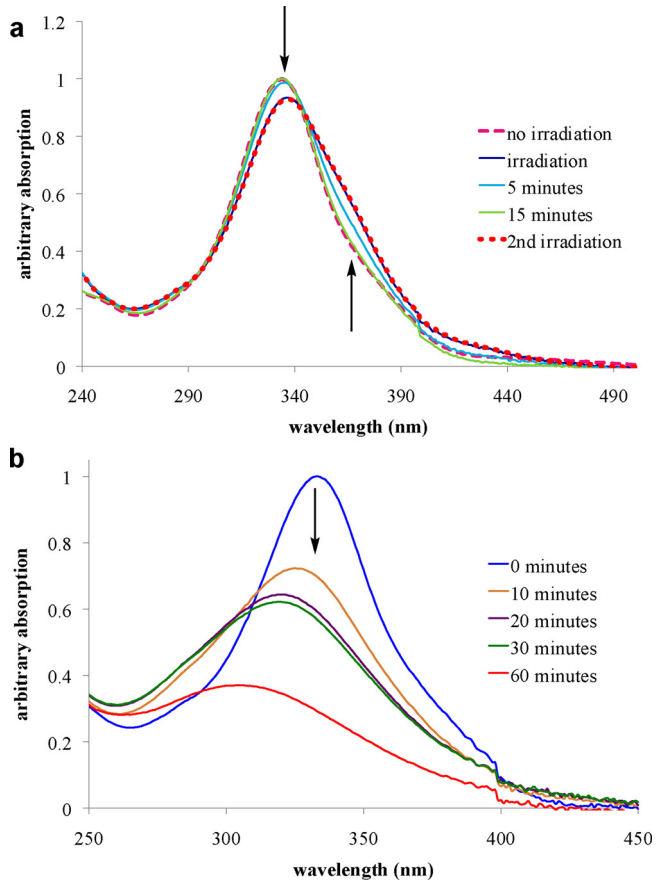

Fig. 7. Photoswitching with 365 nm irradiation (a) and photobleaching with 254 nm irradiation (b) for azo[11]CPP (**4**).

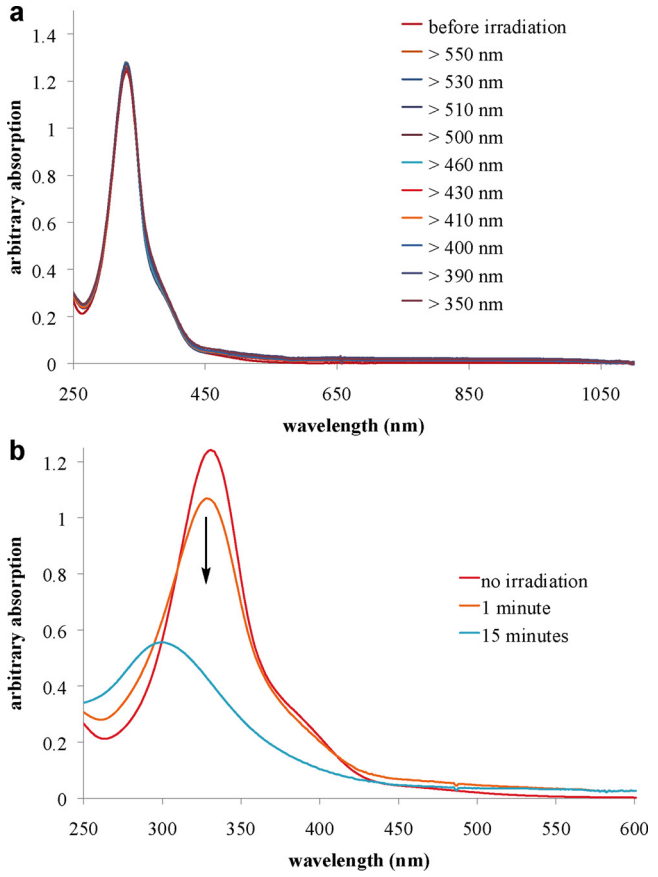

Fig. 8. Photostability at a wide range of irradiation wavelengths (a) and photobleaching with broadband UV irradiation (high pressure mercury arc lamp, IR filter only) (b) for azo[9]CPP (**9**).

(supporting information Fig. S3).

The stability of the *cis* form of **9** and its inactivity as a host for C_{60} was also investigated by NMR experiments. In tetrachloroethane, the *cis* form persists, as evident by the doublet at $\delta = 6.85$ ppm and no appearance of new signals, even when heated to 100 °C (supporting information Fig. S4). Additionally, when sonicated in the presence of excess C_{60} in chloroform or a 1:1 mixture of chloroform and carbon disulfide (to further solubilize the fullerene) and even after 24 h irradiation at 365 nm, we observed no appreciable evidence of complex formation by ^{1}H NMR (Supporting information Fig. S5).

7. Conclusions and outlook

With the data available at this time, the outlook for photoswitchable nanohoops is promising. Though preliminary NMR experiments did not show evidence of complexation when adding C_{60} to a sample of azo [9]CPP with or without irradiation, theoretical data shows that it should form a strong complex once the correct conditions are developed. Similarly, photoisomerization was observed in azo[11]CPP but the synthetic availability of this nanohoop was poor. With initial studies in hand, further development of photoswitchable nanohoops capable of reversible binding of guest molecules is ongoing.

8. Experimental procedures

Full synthesis, photochemistry and characterization details are provided in the accompanying supporting information.

8.1. Azo[11]cycloparaphenylene macrocycle (3)

To a 100-mL flask equipped with a magnetic stir bar was added diboronate **1** (297 mg, 0.264 mmol, 1 equiv), 4,4′-dibromoazobenzene **2** (90.0 mg, 0.264 mmol, 1 equiv), $Pd(OAc)_2$ (27 mg, 0.040 mmol, 0.15 equiv), and ground, oven-dried Cs_2CO_3 (430 mg, 1.32 mmol, 5 equiv). This flask was evacuated and backfilled with dry N_2 five times to exclude moisture and air. Dry dimethylformamide (DMF) (50 mL), and N_2 sparged isopropyl alcohol (5 mL) were added and the mixture was heated to 110 °C while stirring 16 h. After cooling to room temperature, the solution was filtered through a pad of celite and concentrated under reduced pressure. The resulting semisolid was redissolved in 50 ml of dichloromethane (DCM). The solution was washed with H_2O (2 × 50 mL) and brine (50 mL) then dried over sodium sulfate and filtered. Solvent was removed under reduced pressure and the crude solid was chromatographed on silica gel in an ethyl acetate/hexane gradient of increasing polarity to give an orange solid (35 mg, 13%). ^{1}H NMR (500 MHz, Chloroform-d) δ 7.56 (d, J = 8.7 Hz, 4 H), 7.53 (d, J = 3.7 Hz, 4 H), 7.51 (d, J = 3.7 Hz, 4 H), 7.47 (d, J = 8.1 Hz, 4 H), 7.45 (d, J = 8.1 Hz, 4 H), 7.42 (d, J = 4.1 Hz, 4 H), 7.40 (d, J = 4.1 Hz, 4 H), 6.82 (d, J = 8.7 Hz, 4 H), 6.16 (s, 4 H), 6.17 – 6.12 (overlap, 8 H), 3.47 (s, 6 H), 3.45 (s, 6 H), 3.45 (s, 6 H). ^{13}C NMR (126 MHz, Chloroform-d) δ(ppm) 147.56, 142.87, 142.64, 141.50, 140.00, 139.96, 139.94, 133.11, 132.15, 127.89, 127.13, 127.05, 126.50, 126.46, 126.43, 126.41, 126.29, 126.27, 112.81, 74.88, 74.70, 74.13, 52.04, 51.96, 51.92; IR (neat): 3020.0, 2998.8, 2933.2, 2927.5, 2841.4, 1737.6, 1587.2, 1486.9, 1436.7, 1376.9, 1172.9, 1118.5, 1074.2, 1018.2, 948.8, 823.5, 754.0, 723.2, 694.3, 663.4 cm^{-1}.

8.2. Azo[11]cycloparaphenylene (4)

Macrocycle **3** (19 mg, 0.018 mmol, 1.00 equiv) was dissolved in freshly distilled tetrahydrofuran (THF) (5 mL) and cooled to −78 °C under N_2. 1 M sodium naphthalenide in THF (0.40 mL, 0.40 mmol, 20 equiv) was added dropwise to the stirring solution to give a deep blue color. The mixture was stirred for one hour then 1 M I_2 in DCM was added (1.0 mL) followed by saturated sodium thiosulfate in H_2O (2 mL). After warming to room temperature, the solution was extracted with DCM (2 × 5 mL) and concentrated under reduced pressure. The resulting solid was redissolved in 10 ml of DCM. The solution was washed with H_2O (2 × 10 mL) and brine (10 mL) then dried over sodium sulfate and filtered. Solvent was removed under reduced pressure and the crude solid was chromatographed on basic alumina in a THF/petroleum ether gradient of increasing polarity up to 1:5 to give a bold orange solid (6 mg, 39%). ^{1}H NMR (500 MHz, Chloroform-d) δ(ppm) 7.62–7.52 (overlap, 36 H), 7.47 (d, J = 8.6 Hz, 4 H), 6.90 (d, J = 8.6 Hz, 4 H). IR (neat) 2851.29, 2940.96, 2921.68, 2851.29, 1714.44, 1659.47, 1589.08, 1482.05, 1454.09, 1376.95, 1375.98, 1259.35, 1259.31, 1071.28, 809.97 cm^{-1}.

8.3. Bis-azo[11]cycloparaphenylene macrocycle (6)

To a 1-L flask equipped with a magnetic stir bar was added 4,4′-dibromoazobenzene **2** (408 mg, 1.20 mmol, 1 equiv), five-ring diboronate **5** (1.00 g, 1.32 mmol, 1.1 equiv), and SPhos Pd G2 (87.0 mg, 0.120 mmol, 0.05 equiv). This flask was evacuated and backfilled with dry N_2 five times to exclude moisture and air. Dry dioxane (600 mL) was added and the mixture was heated to 90 °C while stirring. Ground, oven-dried K_3PO_4 (300 mg, 1.4 mmol, 2 equiv) in N_2 sparged H_2O (25 mL) was added via syringe and the mixture stirred at 90 °C for 16 h. After cooling to room temperature, the solution was filtered through a pad of celite and concentrated under reduced pressure. The resulting semisolid was redissolved in 150 ml of DCM. The solution was washed with H_2O (2 × 150 mL) and brine (150 mL) then dried over sodium sulfate and filtered. Solvent was removed under reduced pressure and the crude solid was chromatographed on silica gel in an ethyl acetate/hexane gradient of increasing polarity to give a bright orange solid (181 mg, 22%). ^{1}H NMR (300 MHz, Chloroform-d) δ(ppm) 7.79 (d, J = 8.6 Hz, 8 H), 7.70 – 7.42 (overlap, 32 H), 6.19 (d, J = 11.0 Hz, 8 H), 6.14 (d, J = 11.0 Hz, 8 H), 3.52 (s, 12 H), 3.48 (s, 12 H); ^{13}C NMR (151 MHz, Chloroform-d) δ(ppm) 151.34, 143.43, 142.47, 139.49, 133.46, 133.20, 127.15, 126.95, 126.55, 126.16, 123.45, 74.72, 52.08, 52.01; IR (neat): 731.76, 825.06, 907.55, 949.95, 1004.14, 1016.93, 1082.51, 1174.73, 1226.57, 1360.53, 1398.57, 1461.6, 1487.2, 1598.91, 2245.82, 2822.81, 2898.27, 2936.68, 2980.41, 3029.73 cm^{-1}.

8.4. Azo[9]cycloparaphenylene macrocycle (8)

To a 1-L flask equipped with a magnetic stir bar was added 4,4′-dibromoazobenzene **2** (175 mg, 0.514 mmol, 1 equiv), seven-ring diboronate **7** (500 mg, 0.514 mmol, 1 equiv), and SPhos Pd G2 (37.0 mg, 0.0514 mmol, 0.1 equiv). This flask was evacuated and backfilled with dry N_2 five times to exclude moisture and air. Dry dioxane (500 mL) was added and the mixture was heated to 90 °C while stirring. 2 M K_3PO_4 in N_2-sparged H_2O (13 mL, 26 mmol, 50 equiv) was added via syringe and the mixture stirred at 90 °C for 16 h. After cooling to room temperature, the solution was filtered through a pad of celite and concentrated under reduced pressure. The resulting semisolid was redissolved in 150 ml of DCM. The solution was washed with H_2O (2 × 150 mL) and brine (150 mL) then dried over sodium sulfate and filtered. Solvent was removed under reduced pressure and the crude solid was purified by preparative GPC to give a bright orange crystalline solid (85 mg, 22%). When silica gel chromatography is used, an azoxy decomposition product of **8** is obtained but this is not observed with GPC. ^{1}H NMR (600 MHz, Chloroform-d) δ(ppm) 7.42 (d, J = 8.7 Hz, 4 H), 7.40 (d, J = 8.7 Hz, 4 H), 7.37 (d, J = 8.7 Hz, 4 H), 7.34 (d, J = 4.8 Hz, 4 H), 7.32 (d, J = 4.8 Hz, 4 H), 6.80 (d, J = 8.7 Hz, 4 H), 6.14 (s, 4 H), 6.08 (d, J = 10.2 Hz, 4 H), 6.00 (d, J = 10.2 Hz, 4 H), 3.43 (s, 6 H), 3.42 (s, 6 H), 3.36 (s, 6 H); ^{13}C NMR (151 MHz, Chloroform-d) δ(ppm) 153.72, 143.05, 142.99, 142.79, 139.28, 138.71, 130.85, 127.67, 126.81, 126.77, 126.29, 126.25, 126.06, 120.94, 104.16, 74.44, 52.05, 52.01, 51.93; IR (neat): 665.79, 730.71, 756.16, 774.32, 811.49, 828.32, 908.23, 950.28, 1016.15, 1079.73, 1111.83, 1175.55, 1230.26, 1247.31, 1402.92, 1431.92, 1450.22, 1470.18, 1486.2, 1494.24, 1589.03, 1605.35, 2244.81, 2822.44, 2898.61, 2936.15, 2980.76, 3029.34, 3452.37 cm^{-1}.

8.5. Azo[9]cycloparaphenylene (9)

Macrocycle **8** (40 mg, 0.054 mmol, 1 equiv) was dissolved in freshly distilled THF (20 mL) and cooled to −78 °C under N_2. 0.25 M sodium naphthalenide in THF (3.21 mL, 0.803 mmol, 15 equiv) was added dropwise to the stirring solution to give a deep blue color. The mixture was stirred for one hour then 1 M I_2 in dry DCM was added (2.0 mL) followed by saturated sodium thiosulfate in H_2O (5 mL). After warming to room temperature, the solution was extracted with DCM (2 × 10 mL) and concentrated under reduced pressure. The resulting solid was redissolved in 10 ml of DCM. The solution was washed with H_2O (2 × 10 mL) and brine (10 mL) then dried over sodium sulfate and filtered. Solvent was removed under reduced pressure and the crude solid was chromatographed on silica gel in an DCM/hexanes gradient of increasing polarity up to 1:1 then further purified by preparative GPC to give a crystalline orange solid (22 mg, 57%). ^{1}H NMR (600 MHz, Chloroform-d) δ 7.61 (s, 4 H), 7.57 (d, J = 8.8 Hz, 4 H), 7.53 (d, J = 2.5 Hz, 4 H), 7.51 (d, J = 2.5 Hz, 4 H), 7.50 (d, J = 8.6 Hz, 4 H), 7.47 (d, J = 8.6 Hz, 4 H), 7.45 (d, J = 8.3 Hz, 4 H), 7.41 (d, J = 8.8 Hz, 4 H), 6.84 (d, J = 8.3 Hz, 4 H); ^{13}C NMR (151 MHz, Chloroform-d) δ(ppm) 153.14, 139.24, 138.91, 138.04, 137.84, 127.69, 127.66, 127.59, 127.55, 127.23, 127.03, 127.01, 126.94, 120.86; LRMS (FAB+) *(m/z)*: $[M]^+$ calcd. for $C_{54}H_{36}N_2$, 712.90; found, 714.4.

Competing interests

There are no competing interests to declare.

Acknowledgements

Financial support was provided by the National Science Foundation (CHE-1255219), the Sloan Foundation, the Camille and Henry Dreyfus Foundation, and generous startup funds from the University of Oregon. NMR support was provided by NSF-MRI (CHE-1427987), Oregon BEST, and ONAMI.

Appendix A. Supplementary data

Supplementary material related to this article can be found, in the online version, at doi:https://doi.org/10.1016/j.jphotochem.2019.111878.

References

[1] (a) T. Kawase, N. Fujiwara, M. Tsutumi, M. Oda, Y. Maeda, T. Wakahara, T. Akasaka, Supramolecular Dynamics of Cyclic [6]paraphenyleneacetylene complexes with [60]- and [70]fullerene derivatives: electronic and structural effects on complexation, Angew. Chem. Int. Ed. 43 (2004) 5060–5062;
(b) T. Kawase, H. Kurata, Ball-, bowl-, and belt-shaped conjugated systems and their complexing abilities: exploration of the concave-convex π-π interaction, Chem. Rev. 106 (2006) 5250–5273;
(c) T. Kawase, M. Oda, Complexation of carbon nanorings with fullerenes, Pure Appl. Chem. 78 (2006) 831–839;
(d) T. Kawase, K. Tanaka, N. Shiono, Y. Seirai, M. Oda, Onion-type complexation based on carbon nanorings and a buckminsterfullerene, Angew. Chem. Int. Ed.

(116) (2004) 1754–1756.
[2] (a) T. Iwamoto, Y. Watanabe, T. Sadahiro, T. Haino, S. Yamago, Size-selective encapsulation of C60 by [10]Cycloparaphenylene: formation of the shortest fullerene-peapod, Angew. Chem. Int. Ed. 50 (2011) 8342–8344;
(b) J. Xia, J.W. Bacon, R. Jasti, Gram-scale synthesis and crystal structures of [8]- and [10]CPP, and the solid-state structure of C60@[10]CPP, Chem. Sci. 3 (2012) 3018–3021.
[3] (a) Y. Nakanishi, H. Omachi, S. Matsuura, Y. Miyata, R. Kitaura, Y. Segawa, K. Itami, H. Shinohara, Size-selective complexation and extraction of endohedral metallofullerenes with cycloparaphenylene, Angew. Chem. Int. Ed. 53 (2014) 3102–3106;
(b) T. Iwamoto, Y. Watanabe, H. Takaya, T. Haino, N. Yasuda, S. Yamago, Size- and orientation-selective encapsulation of C70 by cycloparaphenylenes, Chem. Eur. J. 19 (2013) 14061–14068;
(c) H. Ueno, T. Nishihara, Y. Segawa, K. Itami, Cycloparaphenylene-based ionic donor–acceptor supramolecule: isolation and characterization of $Li^+@C60 \subset$ [10]CPP, Angew. Chem. Int. Ed. 54 (2015) 3707–3711.
[4] T. Matsuno, S. Sato, R. Iizuka, H. Isobe, Molecular recognition in curved π-systems: effects of π-lengthening of tubular molecules on thermodynamics and structures, Chem. Sci. 6 (2015) 909–916.
[5] (a) M. Liu, X. Yan, M. Hu, X. Chen, M. Zhang, B. Zheng, X. Hu, S. Shao, F. Huang, Photoresponsive host−Guest systems based on a new azobenzene-containing crytpand, Org. Lett. 12 (2010) 2558–2561;
(b) C. Lin, S. Maisonneuve, R. Métivier, J. Xie, Photoswitchable carbohydrate-based macrocyclic azobenzene: synthesis, chiroptical switching, and multistimuli-responsive self-assembly, Chem. Eur. J. 23 (2017) 14996;
(c) T. Yamamoto, D. Nakamura, G. Liu, K. Nishinaka, A. Tsuda, Synthesis and photoisomerization of an azobenzene-containing tetrapyrrolic macrocycle, J. Photochem. Photobiol. A 331 (2016) 66–75.
[6] A. Ueno, H. Yoshimura, R. Saka, T. Osa, Photocontrol of binding ability of capped cyclodextrin, J. Am. Chem. Soc. 101 (1979) 2779–2780.
[7] S. Shinkai, T. Nakaji, Y. Nishida, T. Ogawa, O. Manabe, Photoresponsive crown ethers. 1. Cis-trans isomerism of azobenzene as a tool to enforce conformational changes of crown ethers and polymers, J. Am. Chem. Soc. 102 (1980) 5860–5865.
[8] F. Puntoriero, P. Ceroni, V. Balzani, G. Bergamini, F. Vögtle, Photoswitchable dendritic hosts: a dendrimer with peripheral azobenzene groups, J. Am. Chem. Soc. 129 (2007) 10714–10719.
[9] O.B. Berryman, A.C. Sather, J. Rebek Jr, A light controlled cavitand wall regulates guest binding, Chem. Comm. 47 (2011) 656–658.
[10] P.A. Bonvallet, M.R. Mullen, P.J. Evans, K.L. Stoltz, E.N. Story, Improved functionality and control in the isomerization of a calix[4]arene-capped azobenzene, Tetrahedron Lett. 52 (2011) 1117–1120.
[11] See supporting information ref. 6 for full citation: Frisch, M.J.; et al., Gaussian 09, Revision D.01. Gaussian Inc.: Wallingford CT, 2009.
[12] (a) E.R. Darzi, T.J. Sisto, R. Jasti, Selective syntheses of [7]-[12]Cycloparaphenylenes using orthogonal suzuki-miyaura cross-coupling reactions, J. Org. Chem. 77 (2012) 6624–6628;
(b) T. Iwamoto, Y. Watanabe, Y. Sakamoto, T. Suzuki, S. Yamago, Selective and random syntheses of [n]Cycloparaphenylenes (n = 8–13) and size dependence of their electronic properties, J. Am. Chem. Soc. 133 (2011) 8354–8361.
[13] R. Siewertsen, H. Neumann, B. Buchheim-Stehn, R. Herges, C. Näther, F. Renth, F. Temps, Highly efficient reversible z−E photoisomerization of a bridged azobenzene with visible light through resolved S1(nπ*) absorption bands, J. Am. Chem. Soc. 131 (2009) 15594–15595.
[14] (a) K. Takaishi, M. Kawamoto, A. Muranaka, M. Uchiyama, Fusion of photochromic reaction and synthetic reaction: photoassisted cyclization to highly strained chiral azobenzenophanes, Org. Lett. 14 (2012) 3252–3255;
(b) M. Han, D. Ishikawa, E. Muto, M. Hara, Isomerization and fluorescence characteristics of sterically hindered azobenzene derivatives, J. Lumin. 129 (2009) 1163–1168.
[15] P.J. Evans, E.R. Darzi, R. Jasti, Efficient room-temperature synthesis of a highly strained carbon nanohoop fragment of buckminsterfullerene, Nat. Chem. 6 (2014) 404–408.
[16] T. Kawase, K. Tanaka, N. Fujiwara, H.R. Darabi, M. Oda, Complexation of a carbon nanoring with fullerenes, Angew. Chem., Int. Ed. 42 (2003) 1624–1628.
[17] Y. Norikane, N. Tamaoki, Photochemical and thermal cis/trans isomerization of cyclic and noncyclic azobenzene dimers: effect of a cyclic structure on isomerization, Eur. J. Org. Chem. (2006) 1296–1302.
[18] Y. Zhao, D.G. Truhlar, Size-selective supramolecular chemistry in a hydrocarbon nanoring, J. Am. Chem. Soc. 129 (2007) 8440–8442.
[19] (a) M.A. Ali, M.A. Alam, Theoretical studies on the structure and thermochemistry of cyclicparaphenylenediazenes, RSC Adv. 7 (2017) 40189–40199;
(b) M.A. Ali, M.A. Alam, Novel photoresponsive cyclicparaphenylenediazenes: structure, strain energy, *cis–trans* isomerization, and electronic properties, Photochem. Photobiol. Sci. (2019), https://doi.org/10.1039/C8PP00502H (advance article).
[20] C.P. Joshua, V.N.R. Pillai, Photochemical cyclodehydrogenation of Lewis acid-conjugates of azobenzenes, Tetrahedron 30 (1974) 3333–3337.
[21] J. Yoshino, A. Furuta, T. Kambe, H. Itoi, N. Kano, T. Kawashima, Y. Ito, M. Asashima, Intensely fluorescent azobenzenes: synthesis, crystal structures, effects of substituents, and application to fluorescent vital stain, Chem. Eur. J. 16 (2010) 5026–5035.